

Association between in-scanner head motion with cerebral white matter microstructure: A multiband diffusion-weighted MRI study

Diffusion-weighted Magnetic Resonance Imaging (DW-MRI) has emerged as the most popular neuroimaging technique used to depict the biological microstructural properties of human brain white matter. However, like other MRI technique, traditional DW-MRI data remains subject to head motion artifacts during scanning. For example, previous studies have indicated that, with traditional DW-MRI data, head motion artifacts significantly affect the evaluation of diffusion metrics. Actually, DW-MRI data scanned with higher sampling rate are important for accurately evaluating diffusion metrics because it allows for full-brain coverage through the acquisition of multiple slices simultaneously and more gradient directions. Here, we employed a publicly available multiband DW-MRI dataset to investigate the association between motion and diffusion metrics with the standard pipeline, tract-based spatial statistics (TBSS). The diffusion metrics used in this study included not only the commonly used metrics (i.e., FA and MD) in DW-MRI studies, but also newly proposed inter-voxel metric, local diffusion homogeneity (LDH). We found that the motion effects in FA and MD seems to be mitigated to some extent, but the effect on MD still exists. Furthermore, the effect in LDH is much more pronounced. These results indicate that researchers shall be cautious when conducting data analysis and interpretation. Finally, the motion-diffusion association is discussed.

1 **Title:** Association between In-scanner Head Motion and Cerebral White Matter Microstructure: A Multiband
2 Diffusion-weighted MRI study

3 **Running head:** Head Motion and White Matter Microstructure

4 **Authors:** Xiang-zhen Kong^{1,2}

5 **Affiliation:** ¹ State Key Laboratory of Cognitive Neuroscience and Learning & IDG/McGovern Institute for
6 Brain Research, Beijing Normal University, Beijing, 100875, China; ² Center for Collaboration and Innovation
7 in Brain and Learning Sciences, Beijing Normal University, Beijing, 100875, China.

8 **Correspondence Author:**

9 Xiang-zhen Kong; 2nd Floor, Brain Imaging Center, 19 Xijiekouwai St, Haidian District, Beijing 100875,
10 China. E-mail: kongxiangzheng@gmail.com

11 Introduction

12 Diffusion-weighted MRI (DW-MRI) has become one of the most popular MRI techniques in brain research, as
13 well as in clinical practice. One key application of DW-MRI is diffusion tractography which can be used for the
14 visualization of white matter (WM) tracts (Golby et al. 2011) and construction of the brain neuroanatomical
15 connectome (Gong et al. 2009). Also, it has become a convenient tool for deriving regional measures of
16 diffusivity and anisotropy. These metrics are believed to reflect biological microstructural properties of the
17 white matter, and have been extensively applied as biological markers for studying WM under normal and
18 clinical conditions (Johansen-Berg 2010; Le Bihan 2003; Le Bihan et al. 2001; Travers et al. 2012).

19 However, like other MRI technique, DW-MRI remains subject to specific biological factors (e.g.,
20 temperature), uncertainty from the scanner (e.g., machine SNR, field shim) and, in particular, motion artifacts.
21 Thus, movement of the head during scanning is undesirable, since it not only displaces the brain matter in space
22 but also interferes with the readout of MR signals. Indeed, recent studies have discovered that head motion may
23 introduce unwanted biases. Ling and his colleagues have shown that head motion is associated with both
24 fractional anisotropy (FA) and mean diffusivity (MD) (the effect is greater for MD) (Ling et al. 2012). A recent
25 study have also found group differences in head motion can induce group differences in white matter tract-
26 specific diffusion metrics, and such effects can be more prominent in some specific tracts than others (Yendiki
27 et al. 2013). However, these studies on head-motion artifacts have employed traditional DW-MRI data with
28 relatively low sampling rate (e.g., 9 s) and hence few gradient directions (e.g., $n = 30$). In fact, previous works
29 have indicated that more unique sampling directions may decrease bias of diffusion metrics (e.g., FA and MD)
30 (Landman et al. 2007; Tijssen et al. 2009). Recently, several promising imaging techniques have been
31 proposed, including MR-encephalography (Zahneisen et al. 2011) and multiband echo planar imaging (Moeller
32 et al. 2010). Using the multiband scanning protocol, sampling across the whole brain at any given time is
33 allowed through the acquisition of multiple slices simultaneously. Hence, additional gradient directions can be
34 acquired in the same scan duration without loss in spatial resolution. Both of the advantages appear to result in
35 evaluating diffusion metrics more accurately, but little is known about the head motion effects on diffusion
36 metrics from the multiband dataset.

37 Here, the primary aim was therefore to investigate the relationship between head motion and diffusion
38 metrics estimated from the multiband dataset. In this study, we examined the two tensor-based metrics most
39 typically reported (i.e., FA and MD). Given the fact that they only reflect diffusion properties solely within the
40 voxel, we also examined a newly proposed model-free inter-voxel metric, referred to as local diffusion

41 homogeneity (LDH) (Gong 2013). We hypothesized that motion effects would be mitigated in the multiband
42 DW-MRI data. It has been suggested that head motion alters the measure of diffusion metrics even after motion
43 and eddy current correction (Ling et al. 2012; Tijssen et al. 2009; Yendiki et al. 2013), and that it may also
44 provide information regarding neuronal processing (Yan et al. 2013a; Yan et al. 2013b). Moreover, LDH is a
45 recently proposed metrics and has not been fully validated yet (Gong 2013). In addition, unlike FA and MD,
46 LDH directly depends on the raw diffusivity series without assuming a prior diffusion model (Gong 2013).
47 Therefore, we also hypothesized that the association between head motion and LDH would be quite different to
48 the tensor-based metrics, and may be more sensitive to motion artifacts. We tested these hypotheses by (1)
49 confirming the test-retest reliability of both diffusion metrics and head motion across scan sessions, and (2) by
50 examining the relationship between the averaged diffusion metrics and head motion. We also examined the
51 relationship in each scan session.

52 **Materials and Methods**

53 **Dataset**

54 The dataset used in this study was from the NKI-RS Multiband Imaging Test-Retest Pilot Dataset (Mennes et
55 al. 2012). There were 20 participants (34.3 ± 14.0 years). For each participant, the DW-MRI scans were
56 performed twice (session 1 and session 2), around one week apart. Diffusion weighted images were collected a
57 standard pulse sequence with 2-mm-thick axial slices and 137 directions: TE 85 ms; TR 2400 ms; b value, 1500
58 s/mm²; flip angle, 90°.

59 **Image Processing**

60 DW-MRI images were processed with FMRIB's Software Library (FSL, <http://www.fmrib.ox.ac.uk/fsl>). Non-
61 brain tissue was removed using the Brain Extraction Tool (BET) with a fractional intensity threshold of 0.2, and
62 then raw DW images were affinely registered to the nonDW image, to partially correct for the effects of motion
63 and eddy currents. Then, by fitting a tensor model at each voxel using DTIFit from the FSL (Smith et al. 2004),
64 we obtained the fractional anisotropy (FA) and mean (MD) diffusivity, used in subsequent TBSS analysis
65 (Smith et al. 2006; Smith et al. 2007).

66 To compare between subjects, the TBSS framework was used. In detail, first, we non-linearly aligned the
67 individual FA maps to FSL's standard 1 mm isotropic FA template (FMRIB58_FA) and averaged them to
68 generate a study specific mean FA map. Next, voxels with an FA > 0.2 in the mean FA map were masked out,
69 and the remainder was thinned to create a white matter "skeleton". The resulting skeleton contained WM tracts
70 common to all subjects. Individual FA maps were then projected onto the mean FA skeleton by filling the
71 skeleton with FA values from the nearest tract center. The same non-linear transformations derived for the FA
72 maps were applied to the MD maps.

73 In terms of the LDH metric, it is a novel model-free metric that defines the regional inter-voxel coherence
74 of diffusion series (Gong 2013). Technologically, LDH is quantified within the neighbors ($n = 27$) via the
75 Kendall's coefficient concordance (KCC), after the estimation of the diffusivity strengths along each gradient
76 direction. To compare between subjects, the LDH maps were also projected onto the WM skeleton mask using
77 the TBSS framework described above. In addition, we used the same approach with different neighbor size
78 (i.e., $n = 7$ and $n = 19$) for quantifying the LDH, and also used another approach for quantifying the regional
79 coherence with information theory (Kong et al., 2014). The results in these cases were all similar to those of the
80 original LDH (data not shown).

81 The DW-MRI data preprocessing and TBSS analysis pipelines were both implemented using Nipype
82 (Gorgolewski et al. 2011), a flexible, lightweight and extensible neuroimaging data processing framework in
83 python. The pipeline for calculating both original and improved LDH was implemented in python.

84 **Assessment of in-scanner head motion**

85 To retrospectively estimate head motion during scanning, DW images were realigned to the non-DW image
86 with FMRIB's Linear Image Registration Tool (FLIRT), and at the same time, an affine transformation matrix
87 was obtained for each image. Then, for each image, the root mean squared (RMS) deviation (Jenkinson et al.
88 2002), a summary statistic of in-scanner head motion, was calculated from its transformation using the tool
89 *rmsdiff* from FSL. Since it summarizes six translational and rotational parameters, the RMS has been widely
90 used in the neuroimaging community. For instance, it has been used in fMRI and DTI data processing to check
91 the extent of head motion and make decisions about cohort formation or matching (e.g., Ikuta et al., 2014;
92 Kochunov et al., 2013; Kong, 2014). Technically, the RMS can be calculated directly from the affine matrices
93 with the formula (1).

94

$$RMS = \sqrt{\frac{1}{5} R^2 \text{Trace}(A^T A) + t^T t} \quad (1)$$

95 In formula (1), R is a radius specifying the volume of interest (R = 80mm, approximately the mean
 96 distance from the cerebral cortex to the center of the head), A is a 3x3 'rotation' matrix and t is a 3x1 column
 97 vector of translation. One thing to note is that since the RMS uses all the information from the affine matrices
 98 (including the shear and scaling, if present), it could include the electrical properties of each participant's head.
 99 Nevertheless, the RMS does provide a sensitive index of in-scanner head motion.

100 Here, the RMS was calculated from 2 transformations of consecutive images (Jenkinson et al. 2002). That
 101 is, in-scanner head motion was measured as the summary measure of head motion relative to the preceding
 102 volume as the previous studies (Satterthwaite et al. 2012; Van Dijk et al. 2012). Finally, head motion was
 103 calculated by averaging the RMS deviations for all volumes.

104 **Test-retest reliability of diffusion metrics and head motion estimate**

105 The voxel-wise test-retest reliability for each diffusion metric was calculated with the intra-class correlation
 106 coefficient (ICC) (Shrout & Fleiss 1979).

107

$$ICC = \frac{BMS - EMS}{BMS + (k - 1) EMS} \quad (2)$$

108 The formula estimates the correlation of the subject signal intensities between sessions, modeled by a two-
 109 way ANOVA, with random subject effects and fixed session effects. In this model, the total sum of squares is
 110 split into subject (BMS), session (JMS) and error (EMS) sums of squares; the k is the number of repeated
 111 sessions. The reliability measure for whole-brain analysis was implemented in python and can be accessed
 112 from Nipype (Gorgolewski et al. 2011). The test-retest reliability for head motion estimate was also calculated
 113 with ICC.

114 **Relationship between In-Scanner Head Motion and Diffusion Metrics**

115 To maximize the signal to noise ratio of head motion estimates, first we calculated the average head motion for
 116 each participant across two sessions. Analogously, for accurate measures of microstructure estimates, the MD,
 117 FA and LDH metrics finally used were also taken from the average of the TBSS results across the two sessions.

118 To examine the possible relationship between head motion and diffusion regional metrics, we conducted a
119 statistical analysis using general linear models (GLMs), for the three metrics respectively, with head motion as
120 the variable of interest. In these models, gender, age and handedness were controlled as confounding
121 covariates. Handedness was included here because it is associated with brain structure and the neural
122 processing of attention, while attention deficit may cause more head motion (e.g., Durston et al., 2003; Schmidt
123 et al., 2013). Voxel-wise statistical analysis was performed with Threshold-Free Cluster Enhancement (TFCE)
124 correction (Smith & Nichols 2009) for multiple comparisons, considering fully corrected p-value < 0.05 as
125 significant. In addition, the same statistical procedure was conducted for both session 1 and session 2
126 respectively.

127 **Results**

128 **Test-retest reliability of diffusion metrics and head motion estimate**

129 All of the diffusion metrics in this study showed relatively high test-retest reliability: FA: Mean ICC = 0.71;
130 MD: Mean ICC = 0.71; LDH: Mean ICC = 0.75. In addition, the magnitude of head motion seemed acceptable
131 (Table 1) and showed medium reliability (ICC = 0.54), which is consistent with previous studies (Van Dijk et
132 al. 2012). Although all of the diffusion metrics, as well as the head motion estimate, are relatively reliable
133 across the two scans, they were not exactly the same due to some random artifacts, including motion artifacts
134 and machine noises. Thus, for accurate measures of this microstructure and the head motion estimate, we first
135 averaged the head motion and diffusion metrics across the two sessions and mainly examined the results with
136 the averaged data.

137 ---insert Table 1. ---

138 **Relationship between the head motion estimate and diffusion metrics**

139 In Table 1, we also show a basic summary of the main head motion results of diffusion metrics across all three
140 analyses.

141 Among the two mostly commonly used regional diffusion metrics (i.e., FA and MD), these results
142 indicated that head motion was mainly associated with the MD values. The degree of head motion was
143 positively associated with increased MD mainly within white matter tracts in left hemisphere, including

144 anterior limb of internal capsule, posterior limb of internal capsule, genu of corpus callosum and body of
145 corpus callosum (Fig. 1). In the current report, we focus on voxels that survived the TFCE correction ($p < 0.05$)
146 (Smith & Nichols 2009) within the whole white matter skeleton. For the analyses examining FA, no voxel
147 survived correction for multiple comparisons.

148 For the analyses examining the inter-voxel diffusion metric (i.e., LDH), we found that wide-spread white
149 matter showed significant negative association with head motion ($p < 0.05$, TFCE corrected; Fig. 1). This
150 association mainly involved the bilateral superior longitudinal fasciculus, body and genu of corpus callosum,
151 cingulum, superior, anterior and posterior corona radiate, retrolenticular part of internal capsule, fornix,
152 cerebral peduncle, middle cerebellar peduncle, right anterior and posterior limb of internal capsule, right
153 external capsule and sagittal stratum.

154 ---insert Fig. 1. ---

155 Overall, with the same criterion of significance ($p < 0.05$, TFCE corrected), we found the most number of
156 motion-related voxels with LDH (34551 voxels, 32.25%) and then MD (2686 voxels, 2.51%). No voxel
157 survived with FA.

158 In addition, we also examined the association between head motion and diffusion metrics with data from
159 the two sessions respectively. Although no voxel survived statistical correction for multiple comparisons ($p <$
160 0.05) in most of the analyses (except LDH in Session 2), there were some voxels that showed a significant
161 trend ($p < 0.10$, TFCE corrected; Fig. 2).

162 ---insert Fig. 2. ---

163 Discussion

164 Like any other MRI technique, DW-MRI signal is subject to head motion artifacts, however, the relationship
165 between diffusion metrics and head motion remains incompletely understood. Previous studies have shown a
166 significant relationship between diffusion metrics and head motion (Ling et al. 2012) with conventional
167 scanning protocol. The current study expands on previous work by exploring the relationship between motion
168 and diffusion metrics (including the recently proposed inter-voxel metric, LDH) with a multiband dataset. We
169 found that the motion effects in FA and MD seems to be mitigated to some extent, but the effect on MD still

170 existed. In addition, the effect is much more pronounced in LDH. Since these results are present following
171 standard processing procedures, researchers shall be cautious when conducting data analysis and interpretation.

172 Previous studies suggested a positive association between motion and MD, with increased magnitude of MD
173 as a result of increased total motion (Ling et al. 2012). The results of this study, with multiband dataset,
174 replicate this finding, as a positive relationship between head motion and the magnitude of MD was present in
175 the left hemisphere tracts. The significant association was mainly located in the deeper white matter (e.g.,
176 corpus callosum and the internal capsule). Interestingly, these tracts have often been reported in the literature to
177 differ between a variety of clinical populations and healthy subjects (Carrasco et al. 2012; Travers et al. 2012).
178 For examining FA, we found no significant relationship between head motion and FA after multiple comparison
179 correction. On the one hand, our findings appear consistent with the previous finding (Ling et al., 2012) that the
180 head motion's bias is more pronounced in MD than FA. But on the other hand, given the reduction of the
181 number of motion-related voxels (multiband dataset: 0 voxel for FA, 2686 voxels for MD; Ling et al., (2012):
182 2422 voxels for FA, 22679 voxels for MD), the motion effect seems to be mitigated in the multiband dataset.
183 This may be due to several advantages of the multiband dataset. First, the multiband dataset was acquired with
184 much more gradient directions than traditional datasets, which would result in more accuracy when evaluating
185 diffusion metrics. Second, the multiband scanning protocol allows full-brain coverage through the acquisition
186 of multiple slices simultaneously. This could avoid displacements of brain within a TR and further mitigate the
187 motion effects. Finally, given the fact that multiband protocol is designed for a relatively high sampling rate
188 (i.e., a shorter TR), motion effects from a shorter duration would be expected to decrease. All these advantages
189 could result in higher accuracy and less irrelevant effects (e.g., head motion) when evaluating diffusion metrics.

190 In addition, we also explored the relationship between head motion and LDH values and found that there
191 were widespread voxels significantly associated to head motion. It's worth noting that with a smaller neighbor
192 sizes ($n = 19$ or $n = 7$) when calculating the LDH, we observed the similar result (number of voxels that
193 survived the TFCE correction: 35570 voxels for $n = 19$; 40425 voxels for $n = 7$). This appears to be quite likely
194 caused by motion artifacts. Indeed, the significant voxels were rarely located in the occipital white matter
195 tracts, where motion artifacts may be much weaker than that in prefrontal lobe when subjects are laying supine.
196 These results suggest that LDH values might be more subject to head motion artifacts. The increased
197 susceptibility to motion may be due to the fact that it is an inter-voxel metric which would be subject to shear in
198 the displacement, and that it is directly calculated with raw diffusivity series. Though previous studies have
199 shown LDH values change during aging, the newly proposed metric has not yet well validated (Gong 2013)
200 and simulation and experimental work is required to confirm the motion-LDH association.

201 So, why does the association between motion and diffusion metrics exist? The dominant view at present is
202 that head motion introduces artifacts into diffusion signals, similar to what has been noted in the fMRI
203 literature (Bullmore et al. 1999; Friston et al. 1996; Hajnal et al. 1994), which influence the calculation of
204 diffusion metrics and further results of cross-subject analysis. A common strategy for controlling motion effects
205 in neuroimaging cross-subject analysis is to regress or match motion estimates (Zuo et al. 2010a; Zuo et al.
206 2012; Zuo et al. 2010b). Another strategy for mitigating head-motion artifacts is to remove time series of high
207 motion, which is called ‘scrubbing’ (Power et al. 2012). However, these strategies have their limitations. On the
208 one hand, scrubbing volumes with high motion could not fundamentally change the relationship between
209 motion and values of diffusion metrics (Ling et al. 2012). On the other hand, they may also reduce the ability to
210 detect a significant effect of interest, and/or introduce sampling bias (Satterthwaite et al. 2012; Wylie et al.
211 2014).

212 While researchers attempt to propose more sophisticated algorithms, there is growing perception in the
213 field that head motion reflects individual differences in psychological traits and clinical conditions. For
214 instance, previous studies showed that head motion was correlated with some psychological and clinical
215 measures, such as the autism symptom severity score (Yendiki et al. 2013). In addition, previous fMRI studies
216 suggest that the association may reflect the neural processing related to head motion (Yan et al. 2013a; Yan et
217 al. 2013b). However, it is important to note that this problem in dMRI would not be as serious as it is in fMRI,
218 since in dMRI the neural processing causing the motion does not directly affect the signal intensity.
219 Nevertheless, these findings do suggest that head motion might not simply be an uncorrelated random variable.

220 Taken together, as articulated previously (Van Dijk et al. 2012; Wylie et al. 2014; Yendiki et al. 2013),
221 these findings demonstrate the significance of developing motion-compensated acquisition methods for DW-
222 MRI and incorporating them into neuroimaging studies in the future. Nevertheless, with current technologies, it
223 appears impossible to perfectly eliminate the motion effects. As a temporary solution, examining both models
224 with and without motion being regressed out will be expected. But in this case, researcher should include both
225 results in the report, rather than just pick a ‘better’ one. Additionally, researcher shall keep in mind that motion
226 does not only influence MRI signals, but also correlated with some meaningful individual differences.
227 Alternatively, replication in an independent sample would be helpful, since the effects of head motion on
228 diffusion metrics are usually random and not specific to some brain regions. Nevertheless, for now, researchers
229 shall be cautious when doing MRI data analysis and interpretation.

230 In sum, the results of this study indicate that, in the multiband diffusion data, there are also significant
231 associations between head motion and diffusion metrics, although the motion effects appear to be mitigated

232 compared to those with traditional dataset. Specifically, head motion was associated with both MD and LDH,
233 and no significant effect was found for FA. Future studies should investigate the association between head
234 motion and diffusion metrics with larger multiband datasets.

235 **References**

- 236 Bullmore ET, Brammer MJ, Rabe-Hesketh S, Curtis VA, Morris RG, Williams SC, Sharma T, and
237 McGuire PK. 1999. Methods for diagnosis and treatment of stimulus-correlated motion in generic brain
238 activation studies using fMRI. *Hum Brain Mapp* 7:38-48.
- 239 Carrasco JL, Tajima-Pozo K, Diaz-Marsa M, Casado A, Lopez-Ibor JJ, Arrazola J, and Yus M. 2012.
240 Microstructural white matter damage at orbitofrontal areas in borderline personality disorder. *J Affect*
241 *Disord* 139:149-153.
- 242 Durston S, Tottenham NT, Thomas KM, Davidson MC, Eigsti I-M, Yang Y, Ulug AM, and Casey BJ.
243 2003. Differential patterns of striatal activation in young children with and without ADHD. *Biol Psychiatry*
244 53:871-878.
- 245 Friston KJ, Williams S, Howard R, Frackowiak RS, and Turner R. 1996. Movement-related effects in
246 fMRI time-series. *Magn Reson Med* 35:346-355.
- 247 Golby AJ, Kindlmann G, Norton I, Yarmarkovich A, Pieper S, and Kikinis R. 2011. Interactive
248 diffusion tensor tractography visualization for neurosurgical planning. *Neurosurgery* 68:496-505.
- 249 Gong G. 2013. Local diffusion homogeneity (LDH): an inter-voxel diffusion MRI metric for assessing
250 inter-subject white matter variability. *PLoS One* 8:e66366.
- 251 Gong G, He Y, Concha L, Lebel C, Gross DW, Evans AC, and Beaulieu C. 2009. Mapping anatomical
252 connectivity patterns of human cerebral cortex using in vivo diffusion tensor imaging tractography. *Cereb*
253 *Cortex* 19:524-536.
- 254 Gorgolewski K, Burns CD, Madison C, Clark D, Halchenko YO, Waskom ML, and Ghosh SS. 2011.
255 Nipype: a flexible, lightweight and extensible neuroimaging data processing framework in python. *Front*
256 *Neuroinform* 5:13.
- 257 Hajnal JV, Myers R, Oatridge A, Schwieso JE, Young IR, and Bydder GM. 1994. Artifacts due to
258 stimulus correlated motion in functional imaging of the brain. *Magn Reson Med* 31:283-291.
- 259 Ikuta T, Shafritz KM, Bregman J, Peters BD, Gruner P, Malhotra AK, and Szeszko PR. 2014.
260 Abnormal cingulum bundle development in autism: a probabilistic tractography study. *Psychiatry Res*
261 221:63-68.
- 262 Jenkinson M, Bannister P, Brady M, and Smith S. 2002. Improved optimization for the robust and
263 accurate linear registration and motion correction of brain images. *Neuroimage* 17:825-841.
- 264 Johansen-Berg H. 2010. Behavioural relevance of variation in white matter microstructure. *Curr Opin*
265 *Neurol* 23:351-358.
- 266 Kochunov P, Du X, Moran LV, Sampath H, Wijtenburg SA, Yang Y, Rowland LM, Stein EA, and Hong
267 LE. 2013. Acute nicotine administration effects on fractional anisotropy of cerebral white matter and
268 associated attention performance. *Front Pharmacol* 4:117.
- 269 Kong, X-Z. (2014). Head motion in children with ADHD during resting-state brain imaging. PeerJ
270 PrePrints, 2.
- 271 Kong X-Z, Zhen Z, Liu J. (2014, April): Measuring Regional Diffusivity Dependency via Mutual
272 Information. Presented at the IEEE International Symposium on Biomedical Imaging. April 29-May 2.
273 2014. Beijing. China.
- 274 Landman BA, Farrell JA, Jones CK, Smith SA, Prince JL, and Mori S. 2007. Effects of diffusion
275 weighting schemes on the reproducibility of DTI-derived fractional anisotropy, mean diffusivity, and
276 principal eigenvector measurements at 1.5T. *Neuroimage* 36:1123-1138.

- 277 Le Bihan D. 2003. Looking into the functional architecture of the brain with diffusion MRI. *Nat Rev*
278 *Neurosci* 4:469-480.
- 279 Le Bihan D, Mangin JF, Poupon C, Clark CA, Pappata S, Molko N, and Chabriat H. 2001. Diffusion
280 tensor imaging: concepts and applications. *J Magn Reson Imaging* 13:534-546.
- 281 Ling J, Merideth F, Caprihan A, Pena A, Teshiba T, and Mayer AR. 2012. Head injury or head motion?
282 Assessment and quantification of motion artifacts in diffusion tensor imaging studies. *Hum Brain Mapp*
283 33:50-62.
- 284 Mennes M, Biswal BB, Castellanos FX, and Milham MP. 2012. Making data sharing work: The
285 FCP/INDI experience. *Neuroimage*.
- 286 Moeller S, Yacoub E, Olman CA, Auerbach E, Strupp J, Harel N, and Ugurbil K. 2010. Multiband
287 multislice GE-EPI at 7 tesla, with 16-fold acceleration using partial parallel imaging with application to
288 high spatial and temporal whole-brain fMRI. *Magn Reson Med* 63:1144-1153.
- 289 Power JD, Barnes KA, Snyder AZ, Schlaggar BL, and Petersen SE. 2012. Spurious but systematic
290 correlations in functional connectivity MRI networks arise from subject motion. *Neuroimage* 59:2142-2154.
- 291 Satterthwaite TD, Wolf DH, Loughead J, Ruparel K, Elliott MA, Hakonarson H, Gur RC, and Gur RE.
292 2012. Impact of in-scanner head motion on multiple measures of functional connectivity: relevance for
293 studies of neurodevelopment in youth. *Neuroimage* 60:623-632.
- 294 Schmidt SL, Simões EN, and Schmidt GJ. 2013. The Effects of Hand Preference on Attention.
295 *Psychology* 4:29-33.
- 296 Shrout PE, and Fleiss JL. 1979. Intraclass correlations: uses in assessing rater reliability. *Psychol Bull*
297 86:420-428.
- 298 Smith SM, Jenkinson M, Johansen-Berg H, Rueckert D, Nichols TE, Mackay CE, Watkins KE,
299 Ciccarelli O, Cader MZ, Matthews PM, and Behrens TE. 2006. Tract-based spatial statistics: voxelwise
300 analysis of multi-subject diffusion data. *Neuroimage* 31:1487-1505.
- 301 Smith SM, Jenkinson M, Woolrich MW, Beckmann CF, Behrens TEJ, Johansen-Berg H, Bannister PR,
302 De Luca M, Drobnjak I, Flitney DE, Niazy RK, Saunders J, Vickers J, Zhang YY, De Stefano N, Brady JM,
303 and Matthews PM. 2004. Advances in functional and structural MR image analysis and implementation as
304 FSL. *Neuroimage* 23:S208-S219.
- 305 Smith SM, Johansen-Berg H, Jenkinson M, Rueckert D, Nichols TE, Miller KL, Robson MD, Jones
306 DK, Klein JC, Bartsch AJ, and Behrens TE. 2007. Acquisition and voxelwise analysis of multi-subject
307 diffusion data with tract-based spatial statistics. *Nat Protoc* 2:499-503.
- 308 Smith SM, and Nichols TE. 2009. Threshold-free cluster enhancement: addressing problems of
309 smoothing, threshold dependence and localisation in cluster inference. *Neuroimage* 44:83-98.
- 310 Tijssen RH, Jansen JF, and Backes WH. 2009. Assessing and minimizing the effects of noise and
311 motion in clinical DTI at 3 T. *Hum Brain Mapp* 30:2641-2655.
- 312 Travers BG, Adluru N, Ennis C, Tromp do PM, Destiche D, Doran S, Bigler ED, Lange N, Lainhart
313 JE, and Alexander AL. 2012. Diffusion tensor imaging in autism spectrum disorder: a review. *Autism Res*
314 5:289-313.
- 315 Van Dijk KR, Sabuncu MR, and Buckner RL. 2012. The influence of head motion on intrinsic
316 functional connectivity MRI. *Neuroimage* 59:431-438.
- 317 Wylie GR, Genova H, Deluca J, Chiaravalloti N, and Sumowski JF. 2014. Functional magnetic
318 resonance imaging movers and shakers: Does subject-movement cause sampling bias? *Hum Brain Mapp*
319 35:1-13.

- 320 Yan C-G, Craddock RC, He Y, and Milham MP. 2013a. Addressing Head Motion Dependencies for
321 Small-World Topologies in Functional Connectomics. *Frontiers in Human Neuroscience* 7:910.
- 322 Yan CG, Cheung B, Kelly C, Colcombe S, Craddock RC, Di Martino A, Li Q, Zuo XN, Castellanos
323 FX, and Milham MP. 2013b. A comprehensive assessment of regional variation in the impact of head
324 micromovements on functional connectomics. *Neuroimage*.
- 325 Yendiki A, Koldewyn K, Kakunoori S, Kanwisher N, and Fischl B. 2013. Spurious group differences
326 due to head motion in a diffusion MRI study. *Neuroimage*.
- 327 Zahneisen B, Grotz T, Lee KJ, Ohlendorf S, Reisert M, Zaitsev M, and Hennig J. 2011. Three-
328 dimensional MR-encephalography: fast volumetric brain imaging using rosette trajectories. *Magn Reson*
329 *Med* 65:1260-1268.
- 330 Zuo XN, Di Martino A, Kelly C, Shehzad ZE, Gee DG, Klein DF, Castellanos FX, Biswal BB, and
331 Milham MP. 2010a. The oscillating brain: complex and reliable. *Neuroimage* 49:1432-1445.
- 332 Zuo XN, Ehmke R, Mennes M, Imperati D, Castellanos FX, Sporns O, and Milham MP. 2012.
333 Network centrality in the human functional connectome. *Cereb Cortex* 22:1862-1875.
- 334 Zuo XN, Kelly C, Di Martino A, Mennes M, Margulies DS, Bangaru S, Grzadzinski R, Evans AC,
335 Zang YF, Castellanos FX, and Milham MP. 2010b. Growing together and growing apart: regional and sex
336 differences in the lifespan developmental trajectories of functional homotopy. *J Neurosci* 30:15034-15043.

Table 1 (on next page)

A basic summary of head motion and the motion effects in three diffusion metrics.

The column Motion includes the averaged motion in the sample. The column Motion-Brain Association includes the summary of motion effects in different diffusion metrics (i.e., FA, MD, and LDH). n.r. indicates null results; Plus sign (+) indicates a positive relationship, while minus (–) indicates a negative relationship. *: $p < 0.10$ TFCE corrected, **: $p < 0.05$ TFCE corrected.

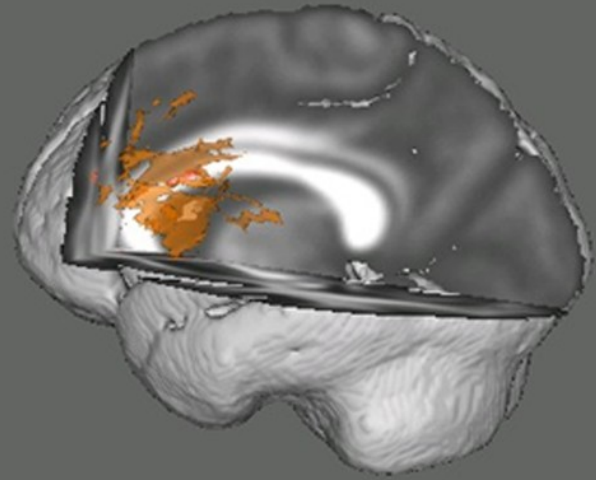
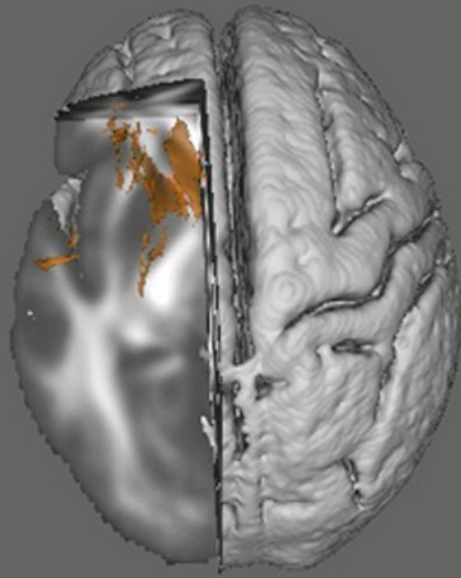
Sample	Motion	Motion-Brain Association		
		FA	MD	LDH
Session 1	1.1(0.32)	n.r.	+*	-*
Session 2	1.26(0.38)	n.r.	+*	-**
Averaged	1.18(0.29)	n.r.	+**	-**

Figure 1

Results from the tract-based spatial statistics (TBSS) analyses depicting the voxels that showed a significant association between head motion diffusion metrics.

Data are presented for the analyses involving both Mean Diffusivity (MD; A) and local diffusion Local Diffusion Homogeneity (LDH; B) as the dependent measure. Participants with higher motion exhibited higher apparent values of MD, but lower LDH. Voxels survived the TFCE correction ($p < 0.05$) across the whole white matter skeleton are displayed.

MD



LDH

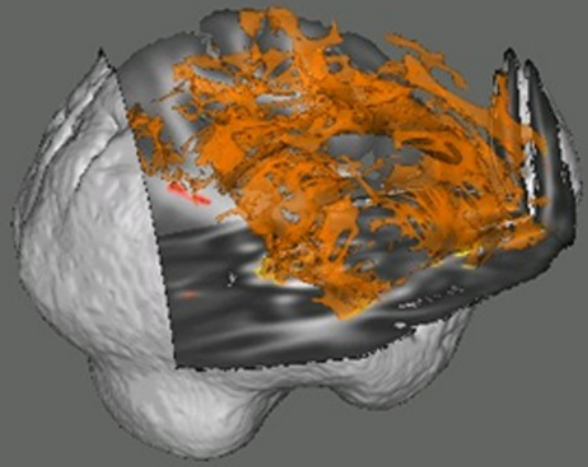
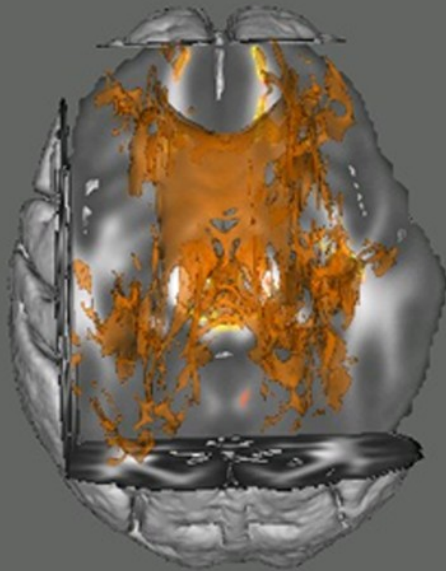


Figure 2

Results from the tract-based spatial statistics (TBSS) analyses depicting the voxels that showed a significant association between head motion diffusion metrics.

Since no voxel that survived statistical correction for multiple comparisons ($p < 0.05$) in most of the analyses (except LDH in Session 2), they are displayed at a more tolerant threshold ($p < 0.10$, TFCE corrected).

